Frontiers in Bioscience Landmark

Front. Biosci. (Landmark Ed) **2025**; 30(10): 44663
https://doi.org/10.31083/FBL44663

Original Research

Deciphering the Role of KIF18A in Osteosarcoma Progression: An Integrative Analysis and Experimental Validation

Zhiqian Gu[1,2,3], Songou Zhang[1], Xudong Hu[2,3], Nanjian Xu[2,3], Yang Wang[2,3], Jian Ruan[2,3], Weihu Ma[2,3,*], Hong Chen[2,3,*]

[1]Health Science Center, Ningbo University, 315211 Ningbo, Zhejiang, China
[2]Department of Orthopaedics, Ningbo No.6 Hospital, 315040 Ningbo, Zhejiang, China
[3]Ningbo Clinical Research Center for Orthopedics, Sports Medicine & Rehabilitation, 315040 Ningbo, Zhejiang, China
*Correspondence: Weihu_ma@163.com (Weihu Ma); chenhong_6612@aliyun.com (Hong Chen)
Academic Editor: Elisa Belluzzi
Submitted: 9 July 2025 Revised: 14 October 2025 Accepted: 17 October 2025 Published: 29 October 2025

Abstract

Background: Osteosarcoma (OS) is a highly aggressive primary bone malignancy with a prominent propensity for metastasis. The identification of the key molecular drivers for OS progression is paramount to developing effective therapies. Although kinesin family member 18A (*KIF18A*) has previously been suggested to play a role as a potential oncogene in the development and metastatic progression of several types of cancer, little is known about its exact functional role in OS. **Methods**: OS datasets were retrieved from the GSE126209 database and the TARGET dataset, with a focus on expression data of kinesin family genes. Differential expression analysis of these genes was conducted using R, comparing tumor tissues to paired adjacent non-tumor tissues, as well as between metastatic and non-metastatic cases. In order to illuminate the functional mechanism, pathway enrichment analysis was executed through Gene Set Enrichment Analysis (GSEA), and the tumor immune microenvironment composition was analyzed comprehensively using the CIBERSORT algorithm. Functional experiments were conducted to investigate the effects of OS *KIF18A* on cell behaviors. *In vivo* experiments were used to identify the function of *KIF18A* on tumor growth. In addition, drug sensitivity profiling and analysis of the lncRNA-mediated regulatory network were implemented to seek possible therapeutic relevance. **Results**: Analysis of the kinesin family gene expression in the GSE126209 OS dataset revealed that *KIF18A* is markedly upregulated in tumor tissues compared to normal counterparts. Further analysis of the TARGET database indicated that elevated *KIF18A* expression is associated with metastatic OS, a finding that was validated using clinical samples from OS patients. Our functional assay indicated that *KIF18A* increased proliferation, invasion, and migration activity of OS cells *in vitro* and inhibited apoptosis. In line with this, the knockdown of *KIF18A* remarkably suppressed tumor growth in OS xenograft models *in vivo*. Pathway enrichment analysis revealed dysregulation of several key signaling pathways associated with *KIF18A* expression, providing mechanistic insights into its oncogenic role. Immune profiling indicated that high *KIF18A* expression was linked to an immunosuppressive tumor microenvironment. Furthermore, drug sensitivity analysis indicated that lower *KIF18A* expression was associated with a higher sensitivity to lapatinib. Additionally, a set of lncRNAs associated with *KIF18A* expression was identified, implicating potential regulatory networks involved in OS progression. **Conclusion**: This study reveals that *KIF18A* is upregulated in OS, particularly in metastatic cases, and is linked to poor clinical outcomes. Functional experiments confirm that *KIF18A* promotes proliferation, migration, and invasion of OS cells while suppressing apoptosis. *In vivo* experiments reveal that *KIF18A* knockdown strongly inhibits tumor growth. *KIF18A* expression correlates with dysregulation of key oncogenic pathways, an immunosuppressive microenvironment, and potential immunotherapy resistance. These results highlight *KIF18A*'s role as a pivotal oncogene in OS progression and suggest its promise as both a prognostic biomarker and a therapeutic target.

Keywords: OS; *KIF18A*; biological; immune; apoptosis; *in vivo*

1. Introduction

Osteosarcoma (OS) is a primary malignant bone tumour which is mainly formed on the metaphyseal area of a long bone adjacent to joint, the femur, tibia and humerus [1,2]. Although most frequently diagnosed in children and adolescents, OS can occur across all age groups [3]. The etiology is still not completely clear but the emerging evidence points to a genotype-environment interaction for the cause of the disease [4,5]. Clinically, patients commonly present with localized bone pain, palpable mass or swelling, and impaired mobility in the affected limb [6]. Pain typically intensifies with disease progression and is often exacerbated at night [7]. An early diagnosis and timely treatment are crucial to clinical outcomes [8]. The standard current management uses a multimodal approach of neoadjuvant chemotherapeutic agents, surgical resection and radiotherapy, in a selection of patients [9]. Surgical goals include complete tumor excision with limb-salvage preservation whenever feasible, whereas systemic therapies aim to eradicate micrometastases and reduce the risk of recurrence [10].

Although remarkable therapeutic improvements have been achieved in recent years, prognosis of patients diagnosed with an advanced or metastatic OS remains poor and thus there remains a desperate unmet clinical need [11]. Ongoing studies towards new therapeutic approaches–including targeted and biologically informed–are thus crucial in order to optimize survival for this type of tumors and to increase patient quality of life. The kinesin superfamily proteins (KIFs) constitute one of the classes of ATP–dependent motor proteins that drive intracellular transport and regulate cell dynamics by moving along microtubules driven by the hydrolysis of ATP [12,13]. Isoforms of these proteins have been linked to organelle, vesicle, and macromolecule trafficking and are key in governing processes that are important for the cell such as mitosis, meiosis, and neurite outgrowth [13,14]. In cancer, KIFs have emerged as important regulators due to their involvement in driving cell proliferation, migration, and invasion [15]. Dysregulation of specific KIF family members has been implicated in tumorigenesis, contributing to malignant phenotypes and disease progression [16]. For example, evidence demonstrates that Forkhead box M1 (FOXM1) promotes hepatocellular carcinoma (HCC) proliferation through direct upregulation of *KIF4A* [17]. Likewise, in different studies *KIF11* was observed to be overexpressed in HCC and to cause tumor growth in octamer-binding transcription factor 4-dependent manner; its inhibition with monastrol was presented as a potential therapeutic avenue [18]. Therefore, understanding the mechanistic roles of KIFs in oncogenesis not only deepens insights into tumor biology but also reveals promising targets for novel anticancer therapies.

KIF18A is an established component of the kinesin-8 family of motor proteins. In mitosis, it uses energy generated from ATP hydrolysis to travel processively along microtubules in the direction of their plus ends [19]. It accumulates in a spatial gradient along spindle microtubules and facilitates precise chromosome alignment at the metaphase plate through the regulation of microtubule dynamics [20]. Genetic or functional inhibition of *KIF18A* results in elongated mitotic spindles, reduced microtubule tension, increased amplitude of chromosome oscillations, and persistent chromosome misalignment [19–21]. Notably, many chromosomal instability (CIN) tumors depend on *KIF18A* to maintain mitotic spindle integrity and sustain proliferative capacity [22]. Consequently, targeting *KIF18A* may inhibit tumor growth and metastasis in chromosomally unstable tumors [23–25]. Moreover, inhibition of *KIF18A* may enhance immune infiltration and activation, improving CD8+ T cell-mediated anti-tumor response [26]. In CIN-driven tumor models, depletion of *KIF18A* leads to mitotic delay, spindle multipolarity, and significantly increased apoptosis [22,27]. *KIF18A* mRNA is frequently overexpressed across diverse malignancies, including breast cancer, lung adenocarcinoma, and cervical cancer [28–30]. Consistent with its essential cellular functions, knockdown of *KIF18A* impairs cancer cell proliferation, tumorigenic potential, and survival in these contexts [28–30].

A recent pan-cancer analysis further confirms widespread upregulation of *KIF18A* across 27 tumor types [16]. In pancreatic adenocarcinoma, *KIF18A* overexpression promotes tumor cell proliferation and migration, an effect potentially driven by mutations in tumor protein 53 (*TP53*) and kirsten rat sarcoma viral oncogene homolog (*KRAS*) [31]. Prior preclinical research has shown that despite the non-essential role of *KIF18A* in the normal cycle of somatic cells, this protein is essential for cancer cell survival, especially in cases involving chromosomal instability, making it an interesting target for therapy [22]. Nonetheless, functional *KIF18A* involvement in OS development has not been thoroughly investigated. Here, we identify *KIF18A* as a key driver of OS progression, with significantly elevated expression observed in metastatic tumors. Functional experiments reveal that *KIF18A* promotes OS cell proliferation, invasion, and migration, while its knockdown induces apoptosis and suppresses xenograft tumor growth. Furthermore, we associate *KIF18A* expression with dysregulated signaling pathways, an immunosuppressive tumor microenvironment, distinct drug sensitivity profiles, and specific long non-coding RNA (lncRNA) interactions. The above observations show multiple roles for *KIF18A* in the development of OS and suggest that it is not only an OS prognostic marker but also a possible therapeutic target.

2. Methods

2.1 Acquisition of Open-Access Data

The OS dataset GSE126209 (https://www.ncbi.nlm.nih.gov/geo/query/acc.cgi?acc=GSE126209) was retrieved from the GEO database (https://www.ncbi.nlm.nih.gov/geo/) and includes 12 tumor samples along with 11 matched adjacent non-tumor tissues. Expression data for 40 kinesin family genes were extracted from this dataset. Differential gene expression between tumor and adjacent tissues was analyzed using R software (v4.3.2). Data visualization was performed with the aid of the ggplot2 (v3.5.2) and ggpubr (v0.6.0) packages in R. Clinical and gene expression data from 89 OS patients were retrieved from the TARGET database (https://www.cancer.gov/ccg/research/genome-sequencing/target), among which survival records were accessible for 86 individuals. Data integration was performed using customized computational scripts developed by the authors. Genes with an average expression level below 0.1 in the integrated transcriptomic dataset were excluded due to their limited biological relevance. The classification of mRNA and lncRNA was conducted using the human genome reference files downloaded from the ENSEMBL database (v113, https://www.ensembl.org). The interaction information between different proteins is directly analyzed online from the STRING database (v12.0,

http://www.string-db.org) and visualized using Cytoscape software (v3.10.2, https://cytoscape.org/) [32].

2.2 Pathway Enrichment Analysis

Gene Set Enrichment Analysis (GSEA) is an algorithm to test if pre-defined gene sets are differentially and co-expressed significantly in two different phenotypes or conditions [33]. This method orders genes across a dataset by their relevance to a particular phenotype or state, and then it evaluates how genes from specific predefined sets are distributed within this ordered list to pinpoint significant overrepresentation. In our research, we utilized GSEA to conduct our biological enrichment analysis, leveraging gene sets from both the MSigDB hallmark gene set collection (v2024.1.Hs, https://www.gsea-msigdb.org/gsea/msigdb/collections.jsp) and Gene Ontology (GO) database (v2024-01-17, https://geneontology.org/). Patients with OS were divided into high- and low-*KIF18A* groups, differential expression analysis was performed and ranked gene list was selected as an input for GSEA.

2.3 Immune Microenvironment Analysis

The CIBERSORT (https://cibersortx.stanford.edu/) algorithm employs a computational technique to deduce the cellular composition within complex tissues through analysis of their gene expression profiles [34]. By using a distinct collection of gene expression markers unique to various cell types, it precisely assesses their relative abundances in a given sample. For our research, we utilized CIBERSORT to perform the immune microenvironment analysis, which allowed us to unravel the detailed constitution of immune cells present in our samples, offering a deeper understanding of the immune dynamics within the disease context examined.

2.4 Single-Cell and Drug Sensitivity Analysis

Single-cell analysis was conducted using data from the Tumor Immune Single-cell Hub (TISCH2, http://tisch.comp-genomics.org/), a publicly available resource designed for the study of tissue-specific cellular heterogeneity [35]. The comprehensive data are given on cell identification, characterization, interaction network that facilitate the systematic study of cellular heterogeneity and how it is regulated in cellular processes. A drug sensitivity analysis was done on the data provided from the Genomics of Drug Sensitivity in Cancer (GDSC) database (https://www.cancerrxgene.org/) [36]. The Tumor Immune Dysfunction and Exclusion (TIDE) database (http://tide.dfci.harvard.edu/) was used for the quantification of the response rate of OS patients on the immunotherapy [37].

2.5 Tissue Samples and Cell Lines

In total, 79 OS tissues and their matched non-cancerous adjacent tissues were collected from the patients undergoing surgical resection of Ningbo No. 6 Hospital within the years ranging from 2014 to 2023. After sectioning, tissue samples were snap-frozen in liquid nitrogen on site, stored at –80 °C and used thereafter. The participants that we included in the study have not yet undergone preoperative radiotherapy or chemotherapy. The written informed consents were provided from all the participants before collection. The utilization of human tissues and related procedures were reviewed and approved by the Ethics Committee of Ningbo No. 6 Hospital (Approval No.: 2025003). The hFOB, MG63, U2OS, and Saos-2 cell lines are obtained from the Cell Bank of Shanghai Branch of Chinese Academy of Sciences, which are cultured in Dulbecco's modified Eagle medium (DMEM; Gibco BRL, Grand Island, NY, USA) supplemented with 10% fetal bovine serum (FBS; Gibco) and 1% antibiotics (Gibco) to support their growth and viability. Cells are grown in 37 °C, 5% CO_2 and 95% relative humidity controlled environment. All cell lines used here are identified by short tandem repeat (STR) profiling and tested mycoplasma negative.

2.6 Quantitative Real-Time PCR (qRT-PCR)

Total RNA was isolated from the tissues and cultured cells with TRIzol reagent (Invitrogen, Carlsbad, CA, USA) and oncolumn DNase I treatment was performed to eliminate genomic DNA contamination. The isolated RNA was following reverse transcribed into complementary DNA (cDNA) with the PrimeScript® RT Reagent Kit (TaKaRa, Dalian, China) following the manufactures recommended protocol. Quantitative real-time PCR (qRT-PCR) assays were conducted using Power SYBR Green PCR Master Mix (Applied Biosystems, Foster City, CA, USA) on real-time PCR detection system. Primer sequences are listed as follows: *KIF18A*, 5′-TGGACTTACTTTACACCAGCCC-3′ (forward) and 5′-GCTGTTTTGTCTTGTTGTCGC-3′ (reverse); GAPDH, 5′-GGAGCGAGATCCCTCCAAAAT-3′ (forward) and 5′-GGCTGTTGTCATACTTCTCATGG-3′ (reverse). The mRNA abundance was normalized to GAPDH and was determined through $2^{-\Delta\Delta Ct}$ method.

2.7 Cell Transfection

Two effective short hairpin RNAs (shRNAs) to specifically knock down *KIF18A* (*sh-KIF18A#1* and #2) were constructed by shRNAs from Beijing Tsingke Biotech Co., Ltd. (Beiing, China) and the non-targeting shRNA (*sh-NC*) as negative control. Lentiviral particles were produced in 293T cells using a three-plasmid packaging construct, the shRNA-expressing plasmids being co-transfected with lentiviral packaging plasmids by Lipofectamine™ 3000 Transfection Reagent (Invitrogen, Waltham, MA, USA). Viral supernatants were harvested 48 h later. The lentiviral particles were used to infect the OS cells in 4 μg/mL polybrene (Sigma-Aldrich, St. Louis, MO, USA) for 72 h, and were selected with 1 μg/mL puromycin for 1 week to obtained the stable *KIF18A*-knockdown cell lines. *KIF18A* overexpression was transfected with *pcDNA3.1-*

KIF18A expression plasmid and empty pcDNA3.1 vector (Hanbio Biotechnology, Shanghai, China), respectively with Lipofectamine™ 3000. We confirm the efficiency of *KIF18A* knockdown and overexpression by quantitative real-time PCR (qRT-PCR) and Western blot analysis. Sequences of the target shRNA was described below:

sh-KIF18A#1: CCCGATTTGTAGAAGGCACAA

sh-KIF18A#2: CGCTTGTTAAAGGATTCTCTT

2.8 Cell Proliferation Assay

Cell proliferation was assessed by Cell Counting Kit-8 (CCK-8) assay, colony formation assay and 5-ethynyl-2′-deoxyuridine (EdU) incorporation assay. In the CCK-8 assay, transfected OS cells (2×10^3 cells per well) were seeded in 96 well microplates (Greiner, Frickenhausen, Germany) and then incubated with the CCK-8 reagent (Dojindo, Shanghai, China) at 10 µL per well for 24, 48 and 72 hrs. The colorimetric changes were measured using a microplate reader (Tecan, Sunrise, Austria) at 450 nm, with higher absorbance values reflecting increased cell proliferation. For the colony formation assay, 200 transfected OS cells were seeded per well into 6-well plates (Greiner) and cultured for 14 days to enable single-cell expansion and colony development. Following incubation, the colonies were fixed using 4% paraformaldehyde and stained with 0.1% crystal violet for visualization. The EdU assay was performed using the Cell-Light EdU Apollo567 *In Vitro* Kit (C10310-1, RiboBio, Guangzhou, China) following the manufacturer's protocol. Briefly, 1×10^5 transfected OS cells were plated in 24-well plates (Greiner) and incubated with EdU solution for 2 hours. Afterwards, cells were fixed with 4% paraformaldehyde for 15 minutes, permeabilized using 0.5% Triton X-100, and then labeled with the Apollo567 reaction mixture (RiboBio) for 30 minutes. Nuclei were counterstained with Hoechst 33342 (RiboBio) for 30 minutes as a positive control. EdU-positive cells were visualized and quantified under an inverted fluorescence microscope (Olympus Corporation, Tokyo, Japan) with five random fields analyzed per sample.

2.9 Transwell Assays

Transwell migration and invasion assays were carried out using Corning Transwell-24-well plates with 8.0 µm Pore Polyester Membrane Insert (Corning, NY, USA). Transfected OS cells (1×10^5 cells in 200 µL serum-free medium) were seeded in the upper chamber with Matrigel (BD Biosciences, Franklin Lakes, NJ, USA) for invasion assay, or without Matrigel for migration assay. The lower chamber was supplemented with 500 µL of DMEM (Gibco BRL, Grand Island, NY, USA) containing 20% FBS (Gibco). Following 24 hours of incubation, cells that had not migrated or invaded through the membrane were gently wiped away from the upper chamber using a cotton swab. Migrated or invaded cells located on the bottom side of the membrane were fixed with 4% paraformaldehyde, stained with 0.1% crystal violet, and analyzed under an inverted microscope. Five randomly selected high-power fields were acquired from each filter and processed using ImageJ (v1.54g, National Institutes of Health, Bethesda, MD USA) for quantitative analysis.

2.10 Wound Healing Assay

Transfected OS cells (1×10^5) were plated into individual wells of 6-well plates (Greiner, Frickenhausen, Germany) and grown to complete confluence. A scratch was created in the cell monolayer using a sterile 200 µL pipette tip, followed by three washes with PBS. The cells were then incubated for 24 hours in Dulbecco's modified Eagle medium (DMEM; Gibco BRL, Grand Island, NY, USA) containing 1% fetal bovine serum (FBS; Gibco). Images were acquired at 0, 12, and 24 h using an inverted microscope. The width of the wound was measured using ImageJ software.

2.11 Apoptosis Analysis

The Annexin V-FITC/PI Apoptosis Detection Kit (556547, BD Biosciences, San Jose, CA, USA) was used following the manufacturer's protocol. Briefly, transfected OS cells (1×10^5) were harvested and washed twice with cold PBS before being resuspended in a $1\times$ binding buffer. The cells were next incubated with 5 µL of Annexin V-FITC and 10 µL of propidium iodide staining solution for 15 minutes at room temperature under light-protected conditions. Following incubation, samples were immediately analyzed by a BD LSRFortessa™ flow cytometer (BD Biosciences, San Jose, USA). All experiments were conducted in three independent replicates.

2.12 Western Blot Analysis

Equal quantities of extracted proteins were resolved by SDS-PAGE using a 10% gel and subsequently transferred onto polyvinylidene difluoride (PVDF) membranes. The membranes were incubated with a 5% (w/v) solution of nonfat dried milk for blocking, followed by overnight incubation at 4 °C with primary antibodies. Following this, the membranes were probed with horseradish peroxidase-conjugated secondary antibody (1:5000, sc-2357, Santa Cruz Biotechnology, Santa Cruz, USA). Protein signals were visualized with an enhanced chemiluminescence (ECL) kit (180-5001, Tanon, Shanghai, China), and the intensity of the bands was quantified using ImageJ software. Primary antibodies were: anti-KIF18A (1:1000, ab251863, Abcam, Cambridge, UK), anti-Bax (1:1000, ab32503, Abcam, Cambridge, UK), anti-Bcl-2 (1:1000, ab59348, Abcam, Cambridge, UK), anti-Cleaved Caspase-3 (1:1000, ab2302, Abcam, Cambridge, UK), anti-PARP1 (1:1000, ab32138, Abcam, Cambridge, UK), anti-Cleaved PARP1 (1:1000, ab32064, Abcam, Cambridge, UK), as well as the internal loading controls anti-β-Actin (1:2500, ab179467, Abcam, Cambridge, UK) and anti-

GAPDH (1:2500, ab9485, Abcam, Cambridge, UK). The experiment was conducted a minimum of three times.

Table 1. Correlation between *KIF18A* Expression and Clinical Features (n = 79).

Variable	*KIF18A* Expression		*p*-value
	Low	High	
Gender			
Male	17	23	0.822
Female	18	21	
Age			
<60	24	27	0.636
≥60	11	17	
Location			
Tibia/femur	16	24	0.500
Elsewhere	19	20	
Tumor Size			
<8	21	13	0.011*
≥8	14	31	
Distant Metastasis			
Absent	23	18	0.041*
Present	12	26	
TNM			
I/II	21	14	0.022*
III/IV	14	30	
Differentiated Degree			
High/middle	22	12	0.002*
Low/undifferentiation	13	32	

Low/high by the sample median. Pearson χ^2 test. *$p < 0.05$ was considered to be statistically significant.
KIF18A, Kinesin family member 18A; TNM, Tumor Node Metastasis.

2.13 In Vivo Assay

Ten BALB/c nude male mice (4–6 weeks old; body weight 18–24 g) were purchased from Shanghai SLAC Laboratory Animal Co., Ltd. (Shanghai, China). They were equally classified into two groups (n = 5 per group), injected subcutaneously with U2OS cells stably transfected with either *sh-KIF18A* or *sh-NC*. 1×10^6 U2OS cells in the logarithmic growth phase were suspended in 100 µL of phosphate-buffered saline (PBS) and subsequently injected subcutaneously into the right axilla of the mice. Tumor size was monitored and recorded every four days. After 20 days, the mice were euthanized via CO_2 asphyxiation at a flow rate between 30% and 70% of the chamber volume per minute, with cervical dislocation carried out afterward to confirm euthanasia. Tumor volume was calculated using the formula (mm^3): tumor volume = length × width^2 × 0.5. The animal use protocol has been reviewed and approved by the Animal Ethics and Welfare Committee (AEWC) of Ningbo University (Approval No.: AEWC-2024-0002).

2.14 Immunohistochemistry (IHC)

IHC was performed as previously described [38]. In brief, xenograft sections from paraffin were incubated at 4 °C in a humid chamber with primary antibodies against Ki-67 (1:500, ab15580, Abcam, Cambridge, UK) and KIF18A (1:500, ab251863, Abcam, Cambridge, UK). The proteins were visualized in situ using the BioGenex Super Sensitive LinkLabel IHC Detection System (BioGenex, Fremont, CA, USA).

2.15 Statistical Analysis

R and GraphPad Prism 10 (San Diego, CA, USA) were applied to statistical analyses of this study. Differences between two groups were analyzed by Student's *t* test and those between multi-groups were analyzed by one-way ANOVA, and the chi-square test was done to analyze the comparison of the rate of the category. Spearman's correlation analysis was done to analyze the correlation of expression levels. Survival curves were depicted with Kaplan-Meier and differences were analyzed by Log-rank test. The data are expressed as mean ± standard deviation (SD). The p-value < 0.05 was recognized as significant.

3. Results

3.1 Identification of the KIF18A in OS

Firstly, we identified the KIFs family in OS patients of the TARGET database and analyzed their underlying protein interaction based on the STRING database (Fig. 1A). Using the cytohubba plugin in Cytoscape software, we noticed that the *KIF20A*, *KIF15*, *KIF6*, *KIF13B*, *KIF16B*, *KIF23*, *KIF11*, *KIF22*, *KIF18A* and KIF2A were the key nodes of the protein-protein interaction network (Fig. 1B). We examined the expression levels of 40 kinesin family genes in the GSE126209 OS dataset by comparing tumor tissues with adjacent non-cancerous tissues (Fig. 1C,D). Analysis revealed that *KIF18A* was significantly overexpressed in cancerous tissues ($p = 0.0009$) (Fig. 1D). Then, we evaluated the expression level of the KIFs family in metastatic (n = 22) and non-metastatic (n = 64) OS patients in TARGET-OS database. We found that all members of the KIF family are not statistically significant in terms of survival analysis (Fig. 1E,F). However, considering the relatively small sample size of the TARGET-OS, we believe this limitation can be relaxed. Therefore, due to the higher expression of *KIF18A* in OS, we chose *KIF18A* for further study. Not surprisingly, we identified that *KIF18A* was upregulated in OS tissues compared with its paired non-tumorous tissues (Fig. 1G) and showed significantly greater expression in metastatic tissues as well (Fig. 1H). To examine the potential correlation between the expression of *KIF18A* and clinical features, we performed an analysis of *KIF18A* expression and some clinical features of 79 patients with OS. According to the mean expression level of *KIF18A*, the samples were divided into 2 groups, the

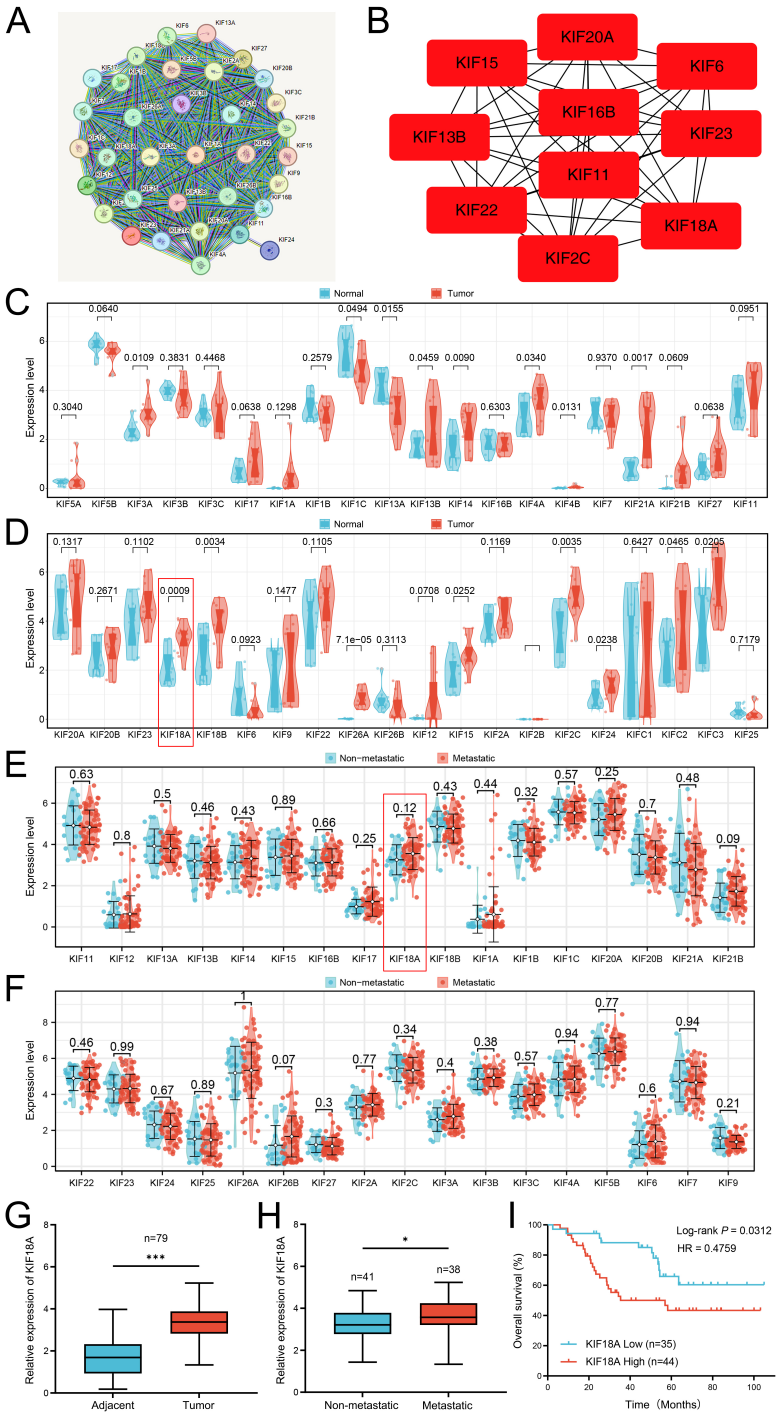

Fig. 1. Identification of KIFs family in the OS patients. (A) The protein-protein interaction network of KIFs family in OS. (B) The key nodes identified by cytoHubba plug-in in the cytoscape software. (C,D) Expression profiling of KIFs family in tumor tissues compared to paired adjacent normal tissues. (E,F) The expression level of KIFs family in metastatic and non-metastatic OS patients. (G) qRT-PCR was used to detect the expression level of *KIF18A* in OS tissues (n = 79) and corresponding adjacent normal tissues (n = 79). (H) qRT-PCR was used to evaluate the expression level of *KIF18A* in OS tissues with (n = 38) or without metastasis (n = 41). (I) Kaplan–Meier analysis was conducted on OS patients categorized by low (n = 35) and high (n = 44) expression levels of *KIF18A*. Statistical analysis for (C,D,G) was conducted using Paired Samples *t*-test, whereas Independent Samples *t*-test was utilized for (E,F,H). Data are shown as mean ± SD. The Kaplan-Meier survival analysis shown in (I) was conducted using the log-rank test. *$p < 0.05$, ***$p < 0.001$. KIFs, kinesin superfamily proteins; OS, Osteosarcoma; *KIF18A,* Kinesin family member 18A; SD, standard deviation. The red boxes illustrated in figures D and E highlight the statistical results associated with *KIF18A*.

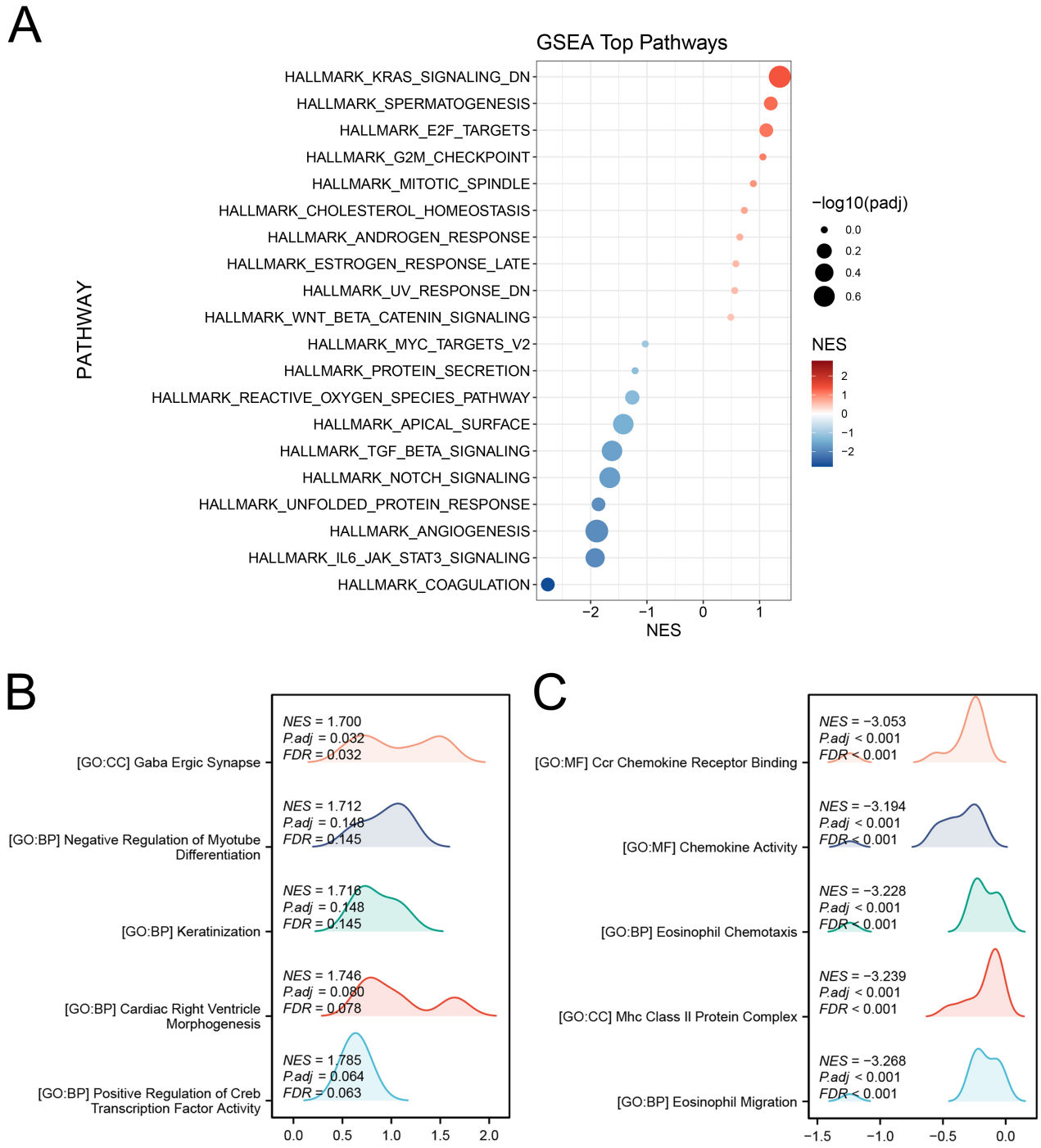

Fig. 2. Biological role of *KIF18A* in OS. (A) GSEA analysis of *KIF18A* based on Hallmark gene set. The color scheme represents the Normalized Enrichment Score (NES), while circle size corresponds to -log$_{10}$(adjusted *p*-value), reflecting the level of statistical significance for each enriched pathway. (B,C) GSEA analysis of *KIF18A* based on GO gene set. GSEA, Gene Set Enrichment Analysis.

KIF18A high expression group and the *KIF18A* low expression group. Table 1 showed that *KIF18A* expression was significantly correlated with different clinical parameters, such as tumor size ($p = 0.011$), distant metastasis ($p = 0.041$), TNM stage ($p = 0.022$), and degree of differentiation ($p = 0.002$). We also evaluated the prognostic meaning of *KIF18A*. Kaplan-Meier analysis revealed that OS with high expression of *KIF18A* showed poor overall survival (Fig. 1I). Thus, the present results imply that *KIF18A* is over-expressed in OS and has a prognostic value for patients with OS.

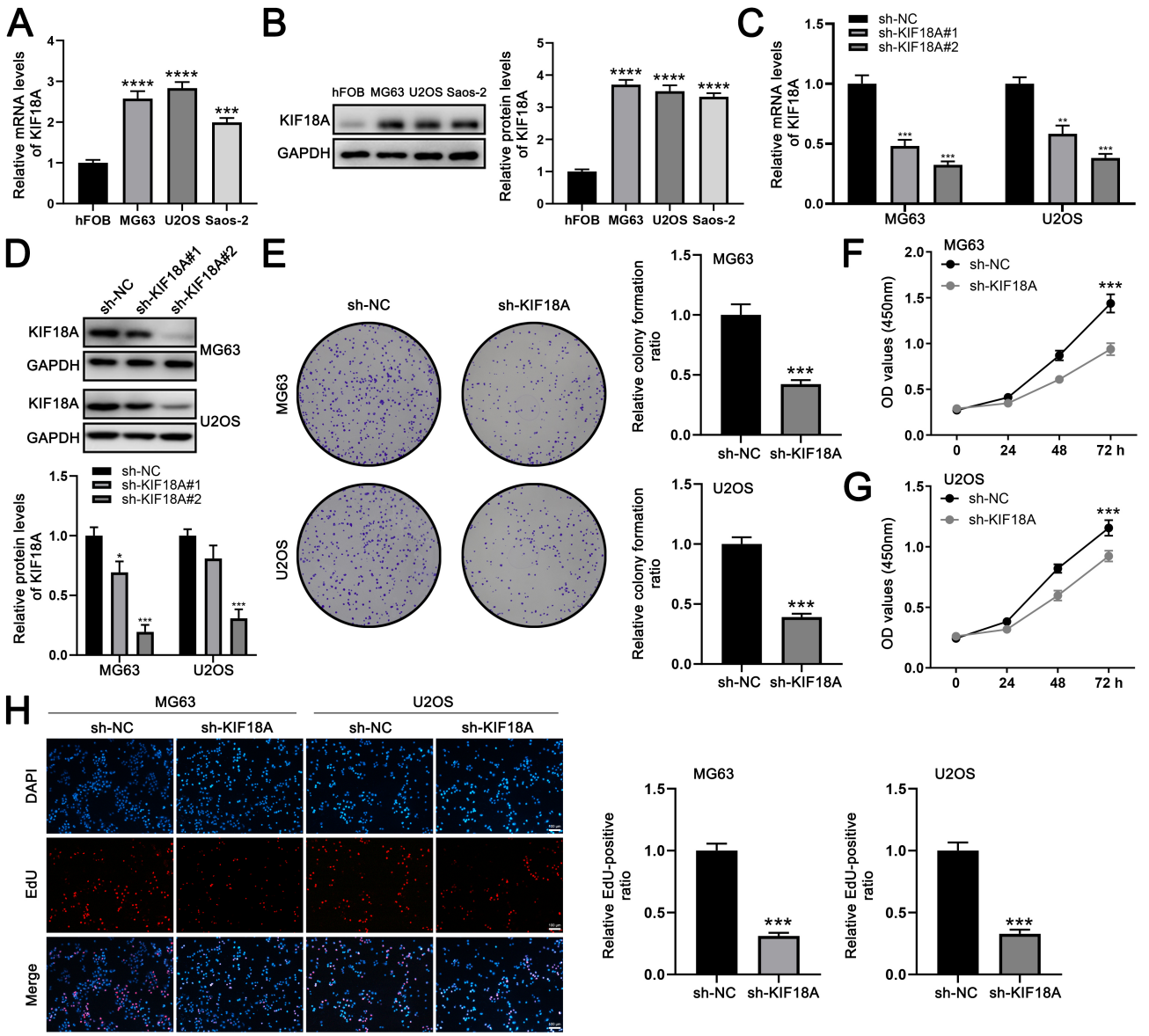

Fig. 3. *KIF18A* promotes the proliferation ability of OS cells. (A) The expression level of *KIF18A* in OS and normal cells. (B) Western blot analysis was performed to detect the expression of the indicated proteins in OS and normal control cell lines. (C) qRT-PCR was used to evaluate the knockdown efficiency of *KIF18A*. (D) Western blot analysis was conducted to evaluate the expression of the indicated proteins in OS cells 48 hours post-transfection with *sh-KIF18A* lentiviruses. (E–G) Colony formation and CCK-8 assays were conducted to compare *KIF18A*-knockdown cells with control cells. (H) EdU assays were conducted in both *KIF18A*-knockdown and control cells. Scale bar: 100 µm. Statistical analysis for (A–E) was conducted using Independent Samples *t*-test. Data are shown as mean ± SD, and all experiments were independently repeated at least three times. $*p < 0.05$, $**p < 0.01$, $***p < 0.001$, $****p < 0.0001$. CCK-8, Cell Counting Kit-8; EdU, 5-ethynyl-2′-deoxyuridine.

3.2 Biological Role of KIF18A in OS

Moreover, we explored the biological function of *KIF18A* in OS patients. GSEA based on the Hallmark gene set revealed that in OS patients exhibiting elevated *KIF18A* expression, several pathways were significantly upregulated, including KRAS signaling, E2F targets, G2M checkpoint, mitotic spindle formation, cholesterol homeostasis, androgen response, and Wnt/β-catenin signaling. Conversely, pathways associated with NOTCH signaling, transforming growth factor-beta (TGF-β) signaling, and interleukin-6 - janus kinase - signal transducer and activator of transcription 3 (IL6-JAK-STAT3) signaling demonstrated downregulation (Fig. 2A). GSEA analysis utilizing the GO gene set suggested that OS patients with high levels of *KIF18A* might experience increased activity related to GABAergic synapses, negative regulation of myotube differentiation, keratinization processes, cardiac right ventricle morphogenesis, and positive regulation of cyclic AMP

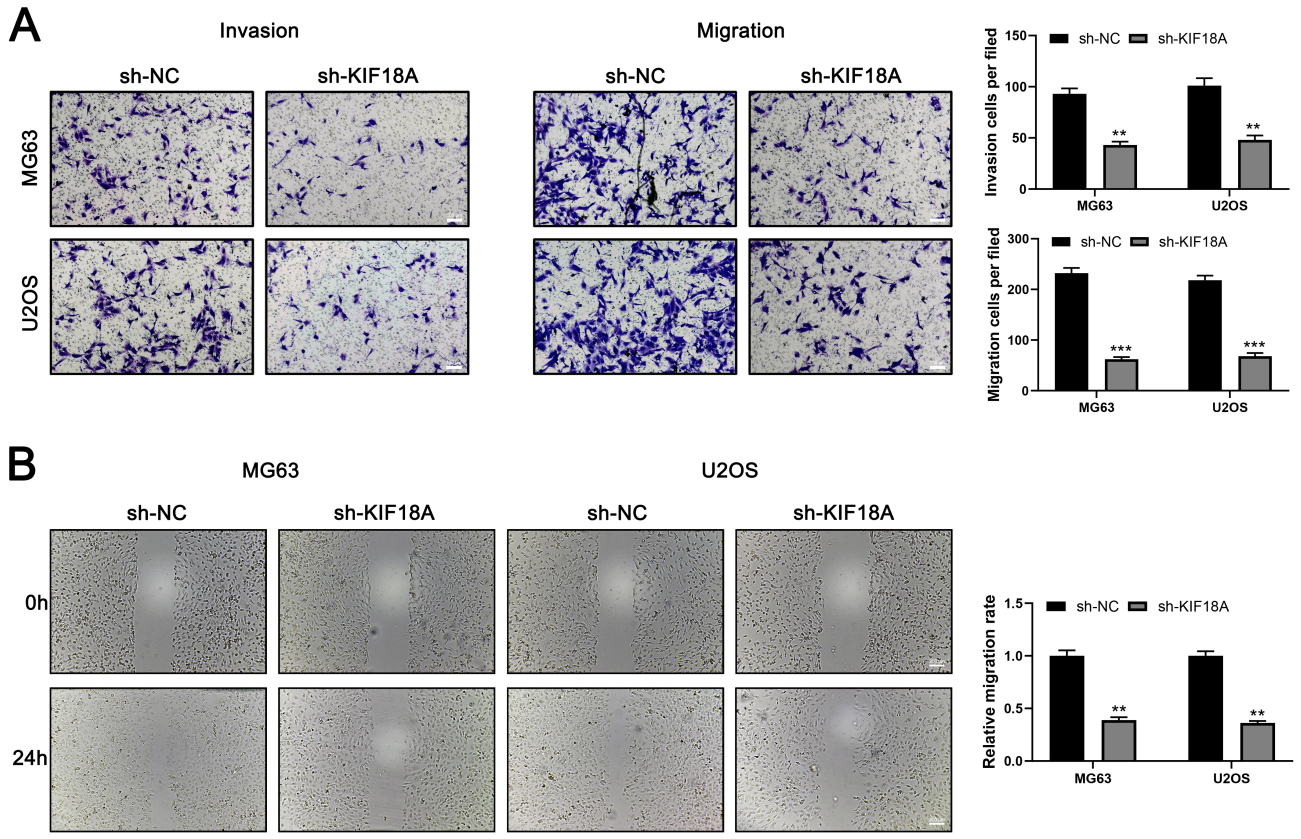

Fig. 4. *KIF18A* promote invasion and migration ability of OS cells. (A) Transwell assay was performed in control and *KIF18A* knockdown cells. Scale bar: 100 μm. (B) Wound-healing assay was conducted in control and *KIF18A* knockdown cells. Scale bar: 200 μm. Statistical analysis for (A,B) was conducted using Independent Samples *t*-test. Data are shown as mean ± SD, and all experiments were independently repeated at least three times. $^{**}p < 0.01$, $^{***}p < 0.001$.

responsive element-binding protein (CREB) transcription factor activity. In contrast, there was a notable reduction in activities involving CCR chemokine receptor binding, chemokine activity, eosinophil chemotaxis migration patterns pertaining to *MHC class II* protein complexes (Fig. 2B,C). Collectively these findings underscore a significant involvement of immune response-associated pathways alongside tumor growth-related mechanisms.

3.3 KIF18A Was Upregulated in OS and Predicted Poor Prognosis

Since the function of *KIF18A* in OS has not been fully elucidated, we first assessed its expression levels in OS cell lines and clinical tissue specimens. Subsequently, we explored the impact of *KIF18A* on the biological behaviors of OS cells. *KIF18A* expression was assessed in OS cell lines in comparison to normal hFOB cells. Both mRNA and protein levels of *KIF18A* were markedly increased in OS cell lines relative to normal controls, with protein expression levels showing a strong correlation to the corresponding mRNA expression trends (Fig. 3A,B). Then, we tried to knock down the *KIF18A* expression and found that the *sh-KIF18A#2* exhibited the highest knockdown efficiency (Fig. 3C,D). Colony formation and CCK8 assay indicated that the inhibition of *KIF18A* can significantly suppress the proliferation ability of OS cells (Fig. 3E–G). Also, the EdU assay indicated a significantly reduced ratio of EdU-positive cells in the *KIF18A* knockdown group compared with the normal group (Fig. 3H). Transwell assay results demonstrated that silencing *KIF18A* significantly suppressed the invasive and migratory capacities of OS cells (Fig. 4A). The wound-healing assay also indicated the same trend (Fig. 4B). Furthermore, we constructed a plasmid for the overexpression of *KIF18A* and observed a significant increase in *KIF18A* levels in OS cells following plasmid transfection (**Supplementary Fig. 1A–C**). *KIF18A* overexpression enhances the proliferation (**Supplementary Fig. 1D–G**), invasion (**Supplementary Fig. 2A**), and migration (**Supplementary Fig. 2B**) of OS cells.

3.4 Knockdown of KIF18A Enhances Apoptosis in OS Cells

Then we transfected *sh-KIF18A* into the OS cells in order to study the effect of *KIF18A* on cellular apoptosis. By cell apoptosis analysis, we observed that the rate of cell apoptosis was increased remarkably in MG63 and

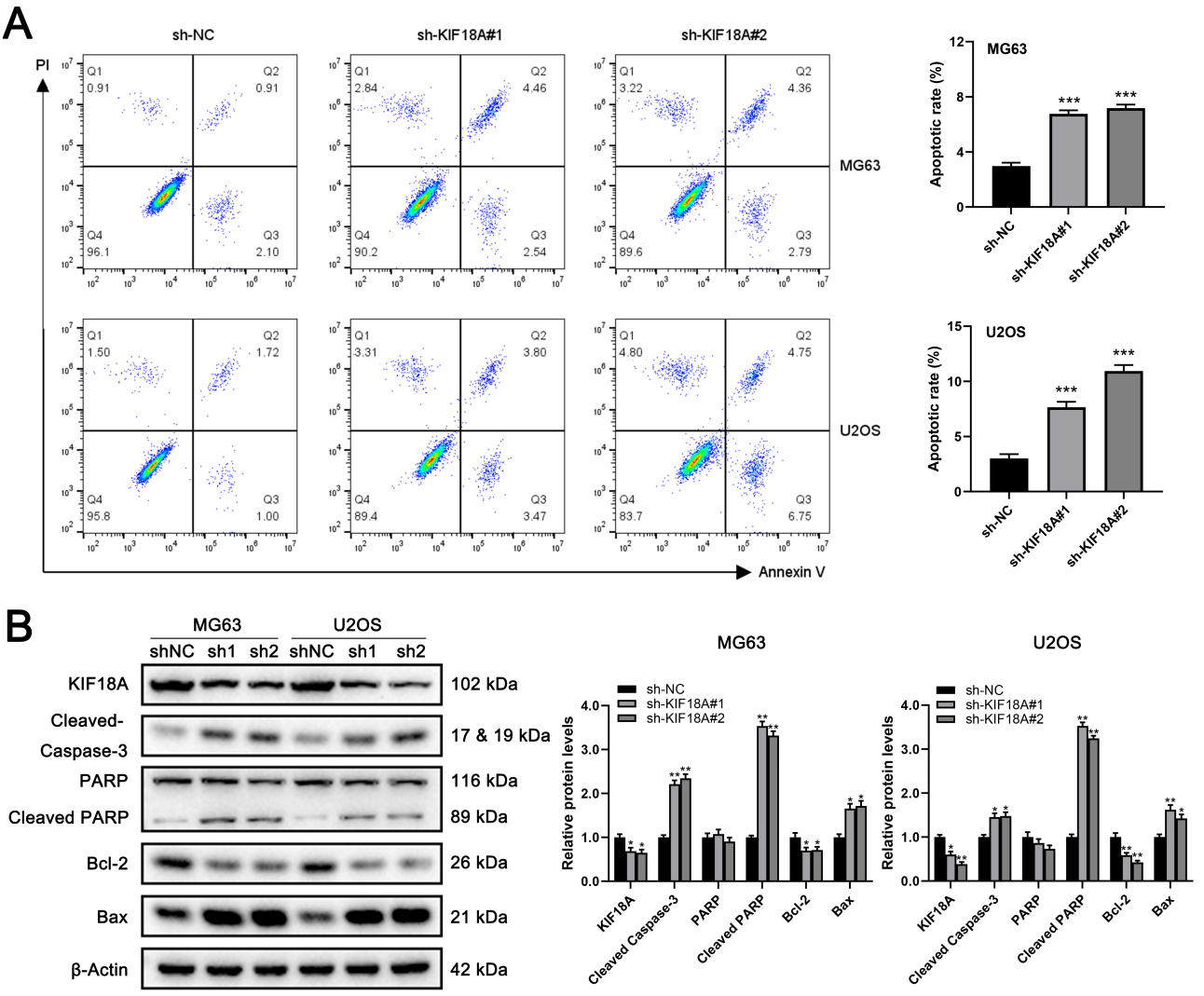

Fig. 5. Knockdown of *KIF18A* promotes apoptosis of OS cells. (A) The apoptosis of MG63 and U2OS cells was assessed through an apoptosis assay, conducted both with and without the silencing of *KIF18A*. (B) Western blotting was performed to evaluate the expression of apoptosis-associated proteins after transfection with *sh-NC* or *sh-KIF18A*. Statistical analysis for A and B was conducted using Independent Samples *t*-test. Data are shown as mean ± SD, and all experiments were independently repeated at least three times. $^{*}p < 0.05$, $^{**}p < 0.01$, $^{***}p < 0.001$.

U2OS cells treated with *KIF18A* knockdown (Fig. 5A). In accordance with these observations, the expressions of the apoptosis-related protein, Cleaved Caspase-3, Cleaved PARP, and Bax, was significantly upregulated in *KIF18A* knockdown cells (Fig. 5B). Conversely, the expression of *Bcl-2* was notably downregulated (Fig. 5B). The data indicate that the downregulation of *KIF18A* expression in MG63 and U2OS cells triggers apoptosis.

3.5 Knockdown of KIF18A Inhibits OS Xenograft Tumor Growth In Vivo

We subsequently examined the impact of *KIF18A* on the growth of OS cells *in vivo*. While all U2OS cells were capable of tumor formation when injected at a density of 1×10^6 cells, the *KIF18A*-knockdown group exhibited a marked decrease in both tumor volume and weight compared to controls (Fig. 6A–C). Tumors derived from *sh-KIF18A*-transfected cells showed an almost twofold reduction in weight relative to the control group (Fig. 6C). Furthermore, the IHC assay indicated that *KIF18A* knockdown led to a decrease in Ki-67 positivity within *in vivo* tumors (Fig. 6D,E). Overall, these results indicate that *KIF18A* knockdown effectively suppresses the progression of human OS xenograft tumors *in vivo*.

3.6 Tumor Microenvironment Analysis

Immune microenvironment has an important impact on the disease progression. To assess the immune landscape of OS, we employed the CIBERSORT algorithm

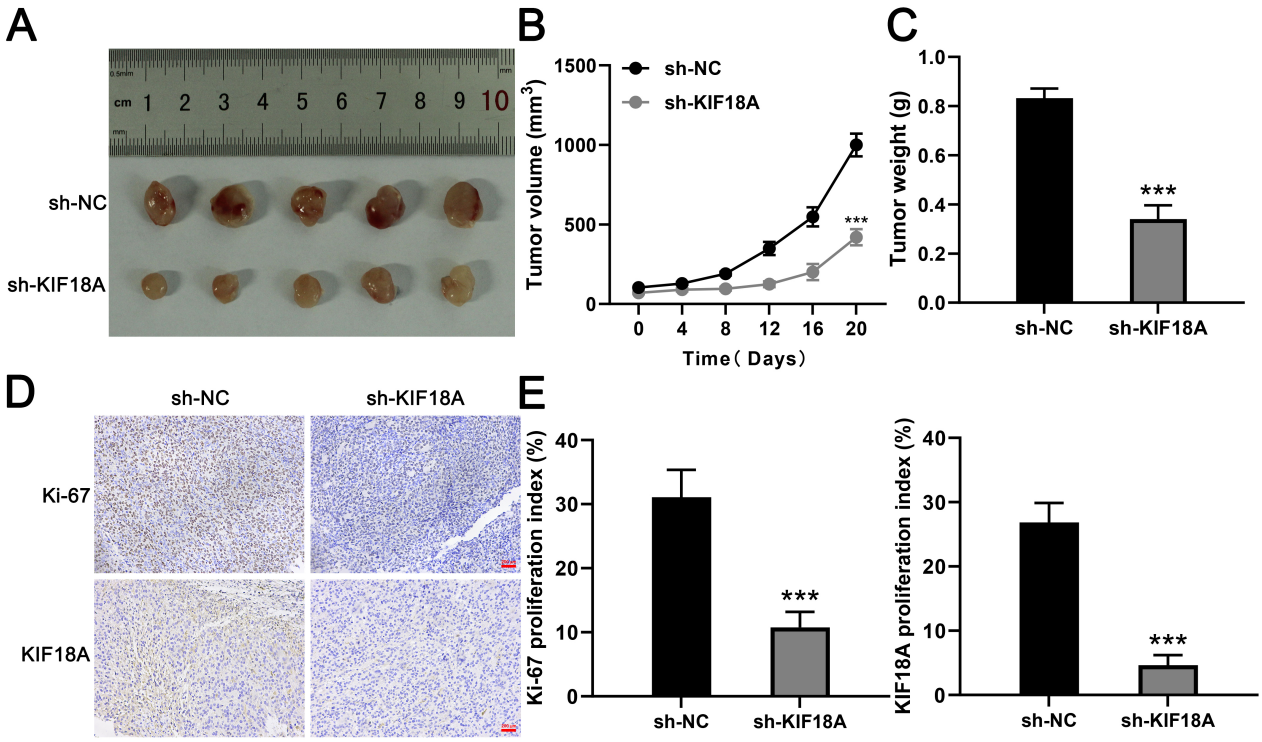

Fig. 6. Knockdown of *KIF18A* inhibits OS cell growth *in vivo*. (A) Typical images of tumors harvested from the *sh-KIF18A* and *sh-NC* groups. (B,C) Tumor volume and weight were assessed in both the *sh-KIF18A* and the *sh-NC* group. (D,E) Representative images illustrate the staining of Ki-67 and *KIF18A* in xenograft sections, with the percentages of positively stained cells indicated. Scale bar: 200 μm. Statistical analysis for (B,C,E) was conducted using Independent Samples *t*-test. Data are shown as mean ± SD, and all experiments were independently repeated at least three times. ***$p < 0.001$.

for quantification (Fig. 7A). Correlation analysis revealed that *KIF18A* was positively associated with CD4+ memory resting T cells, activated NK cells, and CD4+ naïve T cells, but inversely correlated with follicular helper T cells, M2 macrophage, and resting dendritic cells (Fig. 7B). Immune function assessment indicated that patients exhibiting high *KIF18A* expression may have an inhibited immune function, like APC_co_inhibition, CCR, Check_point, HLA, inflammation_promoting and T_cell_co_stimulation (Fig. 7C). Meanwhile, we found that the immune-related gene *HMGB1* was upregulated ($p = 0.00132$) in the OS patients with high *KIF18A* expression (Fig. 7D). Single-cell analysis showed that in the OS microenvironment, *KIF18A* was mainly expressed in the malignant, fibroblasts, osteoblasts and also several immune cells (Fig. 8A,B). Cell interaction results indicated an obvious interaction between fibroblasts and malignant (Fig. 8C). Then, the TIDE algorithm was utilized to estimate the immunotherapy response in OS patients (Fig. 8D). We noticed a positive correlation between *KIF18A* and TIDE score, indicating that patients with high expression of *KIF18A* are more likely to develop immune therapy resistance compared to those with low expression (Fig. 8E). Also, we noticed that *KIF18A* was negatively correlated with immune dysfunction, but positively correlated with MDSC infiltration (Fig. 8F–H).

3.7 Drug Sensitivity Analysis and lncRNA Regulatory Network

Subsequently, we performed a drug sensitivity analysis of common drugs for OS patients. We found that the patients with low *KIF18A* expression might be more sensitive to lapatinib (Fig. 9A). Following this, we tried to identify the lncRNA associated with *KIF18A* with the threshold of |cor| >0.2 and $p < 0.05$ (Fig. 9B). Based on the univariate Cox regression analysis, we found that among these lncRNAs, AC124798.1, MEF2C-AS1, AC147067.1, AC083843.2, SNHG1, NCAM1-AS1, GSEC and AF241728.1 were risk factors, while AC091271.1, AC015819.1, AC005911.1 and AC104561.1 were protective factor (Fig. 9C).

4. Discussion

OS, the most common primary malignant bone tumor, predominantly involves adolescents and young adults with a second incidence rise in aged population seen in conjunction with the disease such as Paget's disease or prior radiation therapy [39]. OS clinically reveals pain and swelling in localized manner mainly in the knee region; specifically distal femur and proximal tibia, and proximal humerus, which are the most commonly affected regions [3]. In ad-

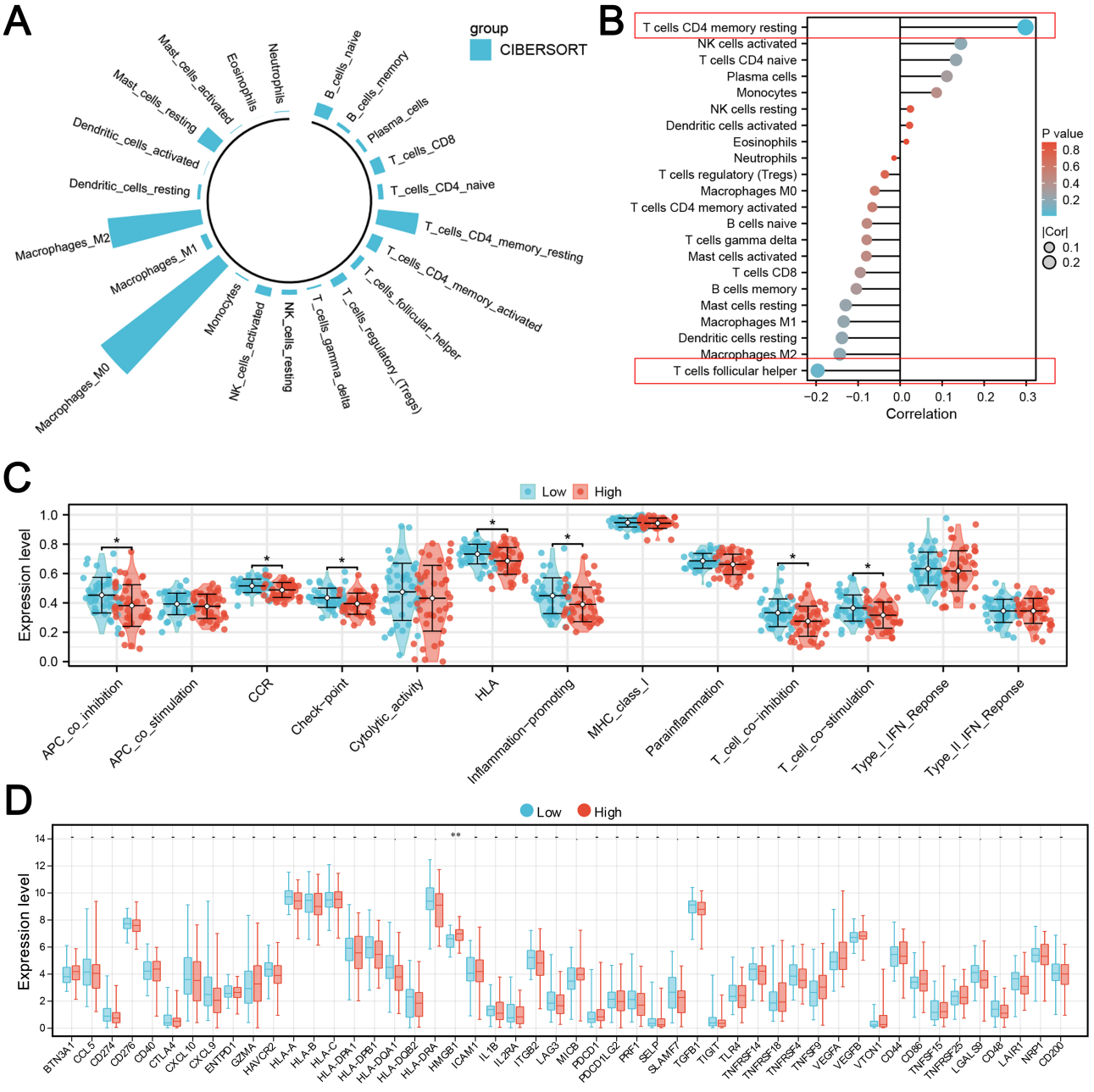

Fig. 7. Immune microenvironment analysis of *KIF18A*. (A) The immune microenvironment of OS patients was quantified using the CIBERSORT algorithm. (B) Correlation between *KIF18A* and quantified immune cells. (C) The immune function terms in patients with high and low *KIF18A* expression. (D) The immune checkpoints level in patients with high and low *KIF18A* expression. Statistical analysis for (C,D) was conducted using Independent Samples *t*-test. Data are shown as mean ± SD, and all experiments were independently repeated at least three times. $*p < 0.05$, $**p < 0.01$. The red box in figure B highlights the most significant correlation.

dition metastases to lungs and bones profoundly affect patient outcomes. Patients with metastatic presentation have much worse prognosis [40]. In spite of emerging therapeutic options, disease in patients with recurrent or metastatic OS has poor prognosis indicating high unmet needs of new therapeutic strategies and deeper knowledge of the biology of OS [41].

This study establishes *KIF18A* as a critical regulator of OS progression, with markedly elevated expression in metastatic cases. *KIF18A* is significantly overexpressed in OS tissues, showing a strong association with disease onset. Comparative analysis reveals higher *KIF18A* levels in metastatic versus non-metastatic patients. Functional studies demonstrate that *KIF18A* drives OS cell proliferation, invasion, and migration. Apoptosis assays and Western blotting confirm that *KIF18A* knockdown induces apoptosis, likely through activation of the extrinsic apoptotic pathway. In mouse xenograft models, silencing *KIF18A* signif-

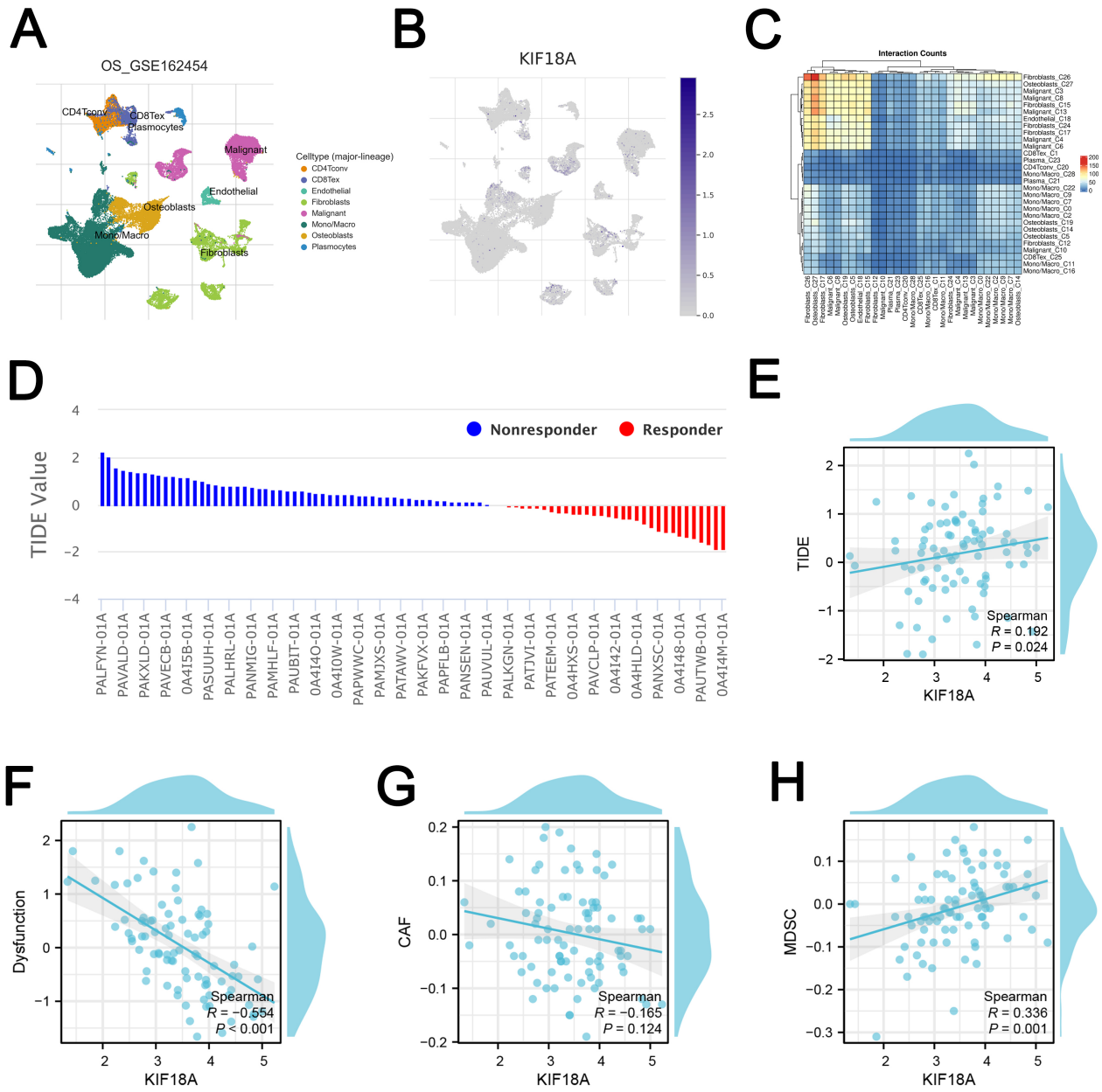

Fig. 8. Single-cell and immunotherapy analysis. (A,B) The single-cell expression of *KIF18A* in OS microenvironment. (C) Cell interaction at single-cell level in OS microenvironment. (D) TIDE analysis was used to quantify the immunotherapy response of OS patients. (E) Correlation between *KIF18A* and TIDE score. (F) Correlation between *KIF18A* and immune dysfunction. (G) Correlation between *KIF18A* and CAFs infiltration. (H) Correlation between *KIF18A* and MDSC infiltration.

icantly suppresses tumor growth. Furthermore, *KIF18A* is associated with alterations in key signaling pathways and the tumor immune microenvironment, suggesting a potential role in modulating immunotherapy response. lncRNAs have emerged as pivotal regulators in the pathogenesis of OS, modulating key cellular processes such as proliferation, metastasis, and chemoresistance through epigenetic, transcriptional, and post-transcriptional mechanisms of gene expression regulation [42,43]. Notably, *KIF18A* expression correlated with sensitivity to certain drugs and exhibited interactions with specific lncRNAs. These findings shed light on *KIF18A*'s multifaceted role in OS pathogenesis, offering insights into its therapeutic potential and highlighting its relevance as a biomarker for prognosis and treatment response.

We demonstrated that patients with high *KIF18A* expression showed various differentially activated signalings from those with low expression. A member of the *RAS* family of oncogenes; the *KRAS* gene participates in the initiation of the tumor [44]. Earlier findings indicate that *KIF18A*

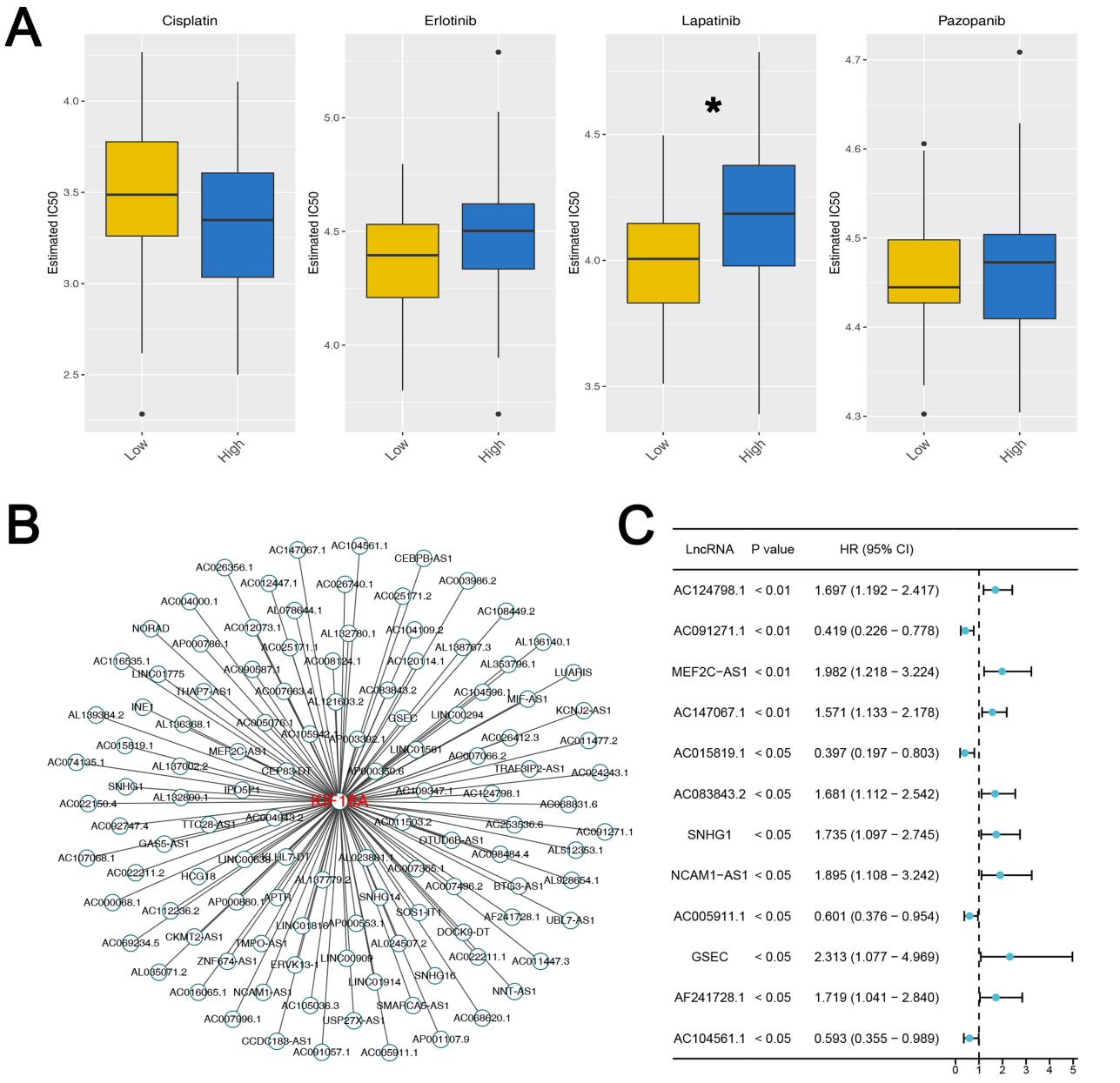

Fig. 9. Drug sensitivity analysis and lncRNA network of *KIF18A*. (A) The IC_{50} difference of specific drugs in patients with high and low *KIF18A* level. Statistical analysis for Figures A was conducted using Independent Samples *t*-test. Data are shown as mean ± SD. *$p < 0.05$. (B) The lncRNA regulatory network of *KIF18A*. (C) Among these regulatory lncRNAs, 12 lncRNAs were identified to have a significant prognosis effect.

enhances the proliferation and migratory capacity of pancreatic adenocarcinoma cells, potentially affected by *KRAS* mutations [31]. A previous study has demonstrated a link between *KRAS* and OS, indicating that *KRAS* may facilitate the growth of OS cells [45]. The abnormal KRAS signaling in the pathogenesis and progression of OS has been evidenced by the disruption of the cell cycle, the apoptosis and the metastasis of the tumors via downstream MAPK/ERK and PI3K/AKT axes [46]. Although *KRAS* mutations may not be as prevalent in OS as in other cancers, the KRAS signaling pathway's role in tumor cell biology suggests it could be a potential target for therapeutic intervention. The G2/M checkpoint is a critical phase in the cell cycle that ensures cells do not enter mitosis (M phase) until their DNA is fully replicated and any DNA damage is repaired after the G2 phase [47]. This checkpoint helps prevent the propagation of damaged DNA, thus avoiding genomic instability and cancer development [48]. In the context of OS, disruptions or dysregulations in the G2/M checkpoint can contribute to the malignant transformation of cells, their proliferation, and the aggressiveness of the tumor. Such dysregulations may also make OS cells more resistant to certain

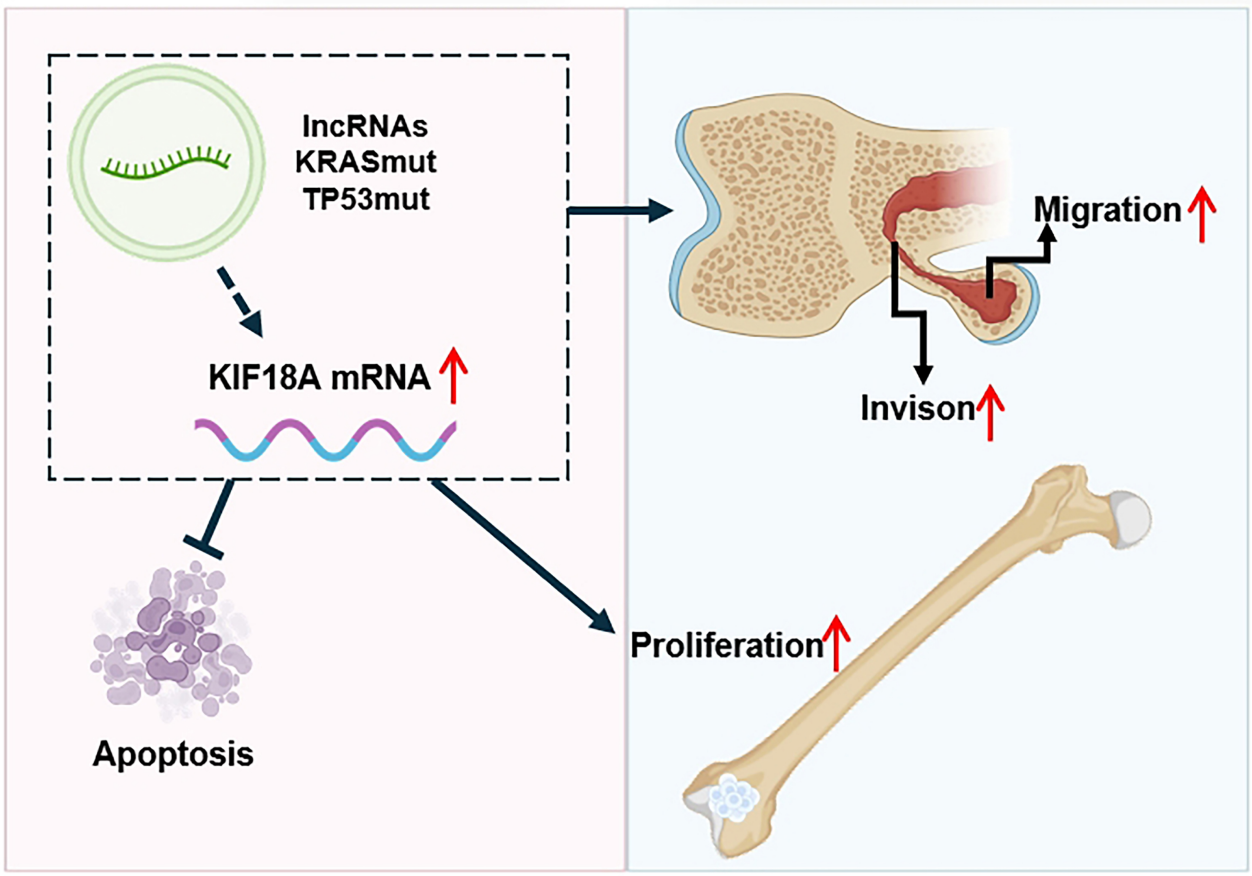

Fig. 10. Schematic diagram of *KIF18A*'s role in OS progression. *KIF18A* is overexpressed in OS, which may be induced by certain lncRNAs and mutations of the *TP53* gene and *KRAS* gene. *KIF18A* is involved in promoting proliferation, invasion and migration of OS cells, also *KIF18A* knockdown induces apoptosis of OS cells. The red arrow indicates a significant increase. This figure created by Adobe Illustrator 2020 (Adobe Systems Incorporated, San Jose, CA, USA).

chemotherapies, as these treatments often target rapidly dividing cells [49]. The NOTCH signaling pathway is a conserved cell signaling in most multicellular organisms that is critical to cellular differentiation, proliferations and apoptosis [50]. Within the realm of oncology, notably in OS, altered NOTCH signaling has been linked to the onset, development, and spread of tumors [51]. Research indicates that NOTCH signaling affects the OS microenvironment by enhancing tumor blood vessel formation and supporting cancer stem cells. These stem cells contribute to a resistance against standard treatments and are linked to a worse outlook for patients [52,53]. In fact, TGF-β signaling is a complicated role in tumor, it acts as tumor suppressor in the early stages of oncogenesis and promoter of tumor progression and metastasis in the latter stages [54]. In OS, TGF-β signaling has been implicated in various aspects of tumor biology, including the promotion of tumor growth, invasion, and metastasis [55]. Overall, these data suggest that the *KIF18A* plays a central role in progression and metastasis in OS. The disparities in pathway activity observed between groups with high versus low *KIF18A* expression could potentially account for the prognostic differences.

Also, we observed that the *KIF18A* expression was significantly associated with CD4+ memory resting T cells positively and follicular helper T cells negatively. On the one hand, CD4+ memory resting T cells are a subset of T cells that have previously encountered antigens and can quickly respond upon re-exposure, playing a crucial role in long-term immune memory [56]. CD4+ memory resting T cells are also related to tumors, including their role in cancer immunity and potential implications for cancer prognosis and therapy [57]. On the other hand, follicular helper T cells play a critical role in the immune system by helping B cells produce antibodies, and their involvement in cancer, including OS, has been an area of growing interest [58]. Finally, the TIDE algorithm constitutes a sophisticated computational framework designed to prognosticate patient responses to immune checkpoint blockade therapies. Considering the variable responses to immune checkpoint blockade therapies directed at the PD-1/PD-L1 and CTLA-4 pathways, TIDE offers a predictive insight, enhancing personalized cancer treatment [59]. Our analysis revealed that patients with low *KIF18A* expression tended to have lower TIDE scores, and that subset of patients may

show a better response to immunotherapy. Patients with low *KIF18A* expression might be more sensitive to lapatinib. Lapatinib is a tyrosine kinase inhibitor that simultaneously inhibits *EGFR* and *HER2* [60]. *EGFR* and *HER2* may be associated with chromosomal instability [61]. The result indicates that *KIF18A* may be an indicator for therapeutic outcomes and prognosis to OS.

5. Conclusion

In conclusion, our study elucidates the pivotal role of *KIF18A* in the initiation, progression, and metastatic behavior of OS, while also exploring its underlying biological functions (Fig. 10). However, some limitations exist in our study. Firstly, a larger sample number is needed to strengthen the robustness of our findings. Secondly, more experiments need to be done to elucidate how *KIF18A* affects the pathogenesis in OS at its specific mechanism level. In the future, investigations into the detailed molecular pathogenesis mediated by *KIF18A*, and assessment of therapeutic interventions against *KIF18A* in preclinical experimental settings remain to be determined.

Availability of Data and Materials

The data used to support the findings of this study are available from the corresponding author upon request.

Author Contributions

Conceptualization, ZG, WM and HC; Data curation, YW and JR; Funding acquisition, ZG; Investigation, NX; Methodology, ZG and SZ; Software, ZG and XH; Writing – original draft, ZG; Writing – review & editing, WM and HC. All authors contributed to editorial changes in the manuscript. All authors read and approved the final manuscript. All authors have participated sufficiently in the work and agreed to be accountable for all aspects of the work.

Ethics Approval and Consent to Participate

The study was carried out in accordance with the guidelines of the Declaration of Helsinki. A written consent was signed by the patients or their families/legal guardians. The use of patients' samples and collection procedures has been reviewed and approved by the Ethics Committee of Ningbo No. 6 Hospital (Approval No.: 2025003). Animal experiments were conducted in accordance with the National Regulations on the Administration of Laboratory Animals (Beijing, China). The animal use protocol has been reviewed and approved by the Animal Ethics and Welfare Committee (AEWC) of Ningbo University (Approval No.: AEWC-2024-0002).

Acknowledgment

Thanks to Laboratory Animal Center of Ningbo University for the technical support.

Funding

This study is supported by Ningbo Natural Science Foundation (202003N4283), Medical Health Science and Technology Project of Zhejiang Provincial Health Commission (2020KY840), Ningbo Clinical Research Center for Orthopedics, Sports Medicine & Rehabilitation (2024L004).

Conflict of Interest

The authors declare no conflict of interest.

Supplementary Material

Supplementary material associated with this article can be found, in the online version, at https://doi.org/10.31083/FBL44663.

References

[1] Ritter J, Bielack SS. Osteosarcoma. Annals of Oncology: Official Journal of the European Society for Medical Oncology. 2010; 21: vii320–5. https://doi.org/10.1093/annonc/mdq276.

[2] Kansara M, Teng MW, Smyth MJ, Thomas DM. Translational biology of osteosarcoma. Nature Reviews. Cancer. 2014; 14: 722–735. https://doi.org/10.1038/nrc3838.

[3] Isakoff MS, Bielack SS, Meltzer P, Gorlick R. Osteosarcoma: Current Treatment and a Collaborative Pathway to Success. Journal of Clinical Oncology: Official Journal of the American Society of Clinical Oncology. 2015; 33: 3029–3035. https://doi.org/10.1200/JCO.2014.59.4895.

[4] Lee JA, Lim J, Jin HY, Park M, Park HJ, Park JW, *et al*. Osteosarcoma in Adolescents and Young Adults. Cells. 2021; 10: 2684. https://doi.org/10.3390/cells10102684.

[5] Jiang ZY, Liu JB, Wang XF, Ma YS, Fu D. Current Status and Prospects of Clinical Treatment of Osteosarcoma. Technology in Cancer Research & Treatment. 2022; 21: 15330338221124696. https://doi.org/10.1177/15330338221124696.

[6] Widhe B, Widhe T. Initial symptoms and clinical features in osteosarcoma and Ewing sarcoma. The Journal of Bone and Joint Surgery. American Volume. 2000; 82: 667–674. https://doi.org/10.2106/00004623-200005000-00007.

[7] McCarville MB. The child with bone pain: malignancies and mimickers. Cancer Imaging: the Official Publication of the International Cancer Imaging Society. 2009; 9 Spec No A: S115–21. https://doi.org/10.1102/1470-7330.2009.9043.

[8] Yoshida A. Osteosarcoma: Old and New Challenges. Surgical Pathology Clinics. 2021; 14: 567–583. https://doi.org/10.1016/j.path.2021.06.003.

[9] Chen C, Xie L, Ren T, Huang Y, Xu J, Guo W. Immunotherapy for osteosarcoma: Fundamental mechanism, rationale, and recent breakthroughs. Cancer Letters. 2021; 500: 1–10. https://doi.org/10.1016/j.canlet.2020.12.024.

[10] Aboulafia AJ, Malawer MM. Surgical management of pelvic and extremity osteosarcoma. Cancer. 1993; 71: 3358–3366. https://doi.org/10.1002/1097-0142(19930515)71:10+<3358::aid-cncr2820711738>3.0.co;2-o.

[11] Xie L, Ji T, Guo W. Anti-angiogenesis target therapy for advanced osteosarcoma (Review). Oncology Reports. 2017; 38: 625–636. https://doi.org/10.3892/or.2017.5735.

[12] Hirokawa N, Noda Y, Tanaka Y, Niwa S. Kinesin superfamily motor proteins and intracellular transport. Nature Reviews. Molecular Cell Biology. 2009; 10: 682–696. https://doi.org/10.1038/nrm2774.

[13] Zhong A, Tan FQ, Yang WX. Chromokinesin: Kinesin super-

family regulating cell division through chromosome and spindle. Gene. 2016; 589: 43–48. https://doi.org/10.1016/j.gene.2016.05.026.

[14] Hirokawa N, Takemura R. Kinesin superfamily proteins and their various functions and dynamics. Experimental Cell Research. 2004; 301: 50–59. https://doi.org/10.1016/j.yexcr.2004.08.010.

[15] Lucanus AJ, Yip GW. Kinesin superfamily: roles in breast cancer, patient prognosis and therapeutics. Oncogene. 2018; 37: 833–838. https://doi.org/10.1038/onc.2017.406.

[16] Liu T, Yang K, Chen J, Qi L, Zhou X, Wang P. Comprehensive Pan-Cancer Analysis of KIF18A as a Marker for Prognosis and Immunity. Biomolecules. 2023; 13: 326. https://doi.org/10.3390/biom13020326.

[17] Hu G, Yan Z, Zhang C, Cheng M, Yan Y, Wang Y, *et al*. FOXM1 promotes hepatocellular carcinoma progression by regulating KIF4A expression. Journal of Experimental & Clinical Cancer Research: CR. 2019; 38: 188. https://doi.org/10.1186/s13046-019-1202-3.

[18] Zhang J, Wei Z, Qi X, Jiang Y, Liu D, Liu K. Kinesin family member 11 promotes progression of hepatocellular carcinoma via the OCT4 pathway. Functional & Integrative Genomics. 2023; 23: 284. https://doi.org/10.1007/s10142-023-01209-7.

[19] Mayr MI, Hümmer S, Bormann J, Grüner T, Adio S, Woehlke G, *et al*. The human kinesin Kif18A is a motile microtubule depolymerase essential for chromosome congression. Current Biology: CB. 2007; 17: 488–498. https://doi.org/10.1016/j.cub.2007.02.036.

[20] Stumpff J, von Dassow G, Wagenbach M, Asbury C, Wordeman L. The kinesin-8 motor Kif18A suppresses kinetochore movements to control mitotic chromosome alignment. Developmental Cell. 2008; 14: 252–262. https://doi.org/10.1016/j.devcel.2007.11.014.

[21] Fonseca CL, Malaby HLH, Sepaniac LA, Martin W, Byers C, Czechanski A, *et al*. Mitotic chromosome alignment ensures mitotic fidelity by promoting interchromosomal compaction during anaphase. The Journal of Cell Biology. 2019; 218: 1148–1163. https://doi.org/10.1083/jcb.201807228.

[22] Marquis C, Fonseca CL, Queen KA, Wood L, Vandal SE, Malaby HLH, *et al*. Chromosomally unstable tumor cells specifically require KIF18A for proliferation. Nature Communications. 2021; 12: 1213. https://doi.org/10.1038/s41467-021-21447-2.

[23] Payton M, Belmontes B, Hanestad K, Moriguchi J, Chen K, McCarter JD, *et al*. Small-molecule inhibition of kinesin KIF18A reveals a mitotic vulnerability enriched in chromosomally unstable cancers. Nature Cancer. 2024; 5: 66–84. https://doi.org/10.1038/s43018-023-00699-5.

[24] Phillips AF, Zhang R, Jaffe M, Schulz R, Carty MC, Verma A, *et al*. Targeting chromosomally unstable tumors with a selective KIF18A inhibitor. Nature Communications. 2025; 16: 307. https://doi.org/10.1038/s41467-024-55300-z.

[25] Mohd Amin AS, Eastwood S, Pilcher C, Truong JQ, Foitzik R, Boag J, *et al*. KIF18A inhibition: the next big player in the search for cancer therapeutics. Cancer Metastasis Reviews. 2024; 44: 3. https://doi.org/10.1007/s10555-024-10225-3.

[26] Liu G, Zhang Y, Cao Z, Zhao Z. Targeting KIF18A triggers antitumor immunity and enhances efficiency of PD-1 blockade in colorectal cancer with chromosomal instability phenotype. Cell Death Discovery. 2025; 11: 130. https://doi.org/10.1038/s41420-025-02437-5.

[27] Cohen-Sharir Y, McFarland JM, Abdusamad M, Marquis C, Bernhard SV, Kazachkova M, *et al*. Aneuploidy renders cancer cells vulnerable to mitotic checkpoint inhibition. Nature. 2021; 590: 486–491. https://doi.org/10.1038/s41586-020-03114-6.

[28] Zhang C, Zhu C, Chen H, Li L, Guo L, Jiang W, *et al*. Kif18A is involved in human breast carcinogenesis. Carcinogenesis. 2010; 31: 1676–1684. https://doi.org/10.1093/carcin/bgq134.

[29] Zhong Y, Jiang L, Lin H, Li X, Long X, Zhou Y, *et al*. Overexpression of KIF18A promotes cell proliferation, inhibits apoptosis, and independently predicts unfavorable prognosis in lung adenocarcinoma. IUBMB Life. 2019; 71: 942–955. https://doi.org/10.1002/iub.2030.

[30] Wang Y, Zhou B, Lian X, Yu S, Huang B, Wu X, *et al*. KIF18A Is a Novel Target of JNK1/c-Jun Signaling Pathway Involved in Cervical Tumorigenesis. Journal of Cellular Physiology. 2025; 240: e31516. https://doi.org/10.1002/jcp.31516.

[31] Nan K, Zhang L, Zou Y, Geng Z, Huang J, Peng Y, *et al*. Integrated Profiling Delineated KIF18A as a Significant Biomarker Associated with Both Prognostic Outcomes and Immune Response in Pancreatic Cancer. ImmunoTargets and Therapy. 2025; 14: 123–138. https://doi.org/10.2147/ITT.S497284.

[32] Szklarczyk D, Kirsch R, Koutrouli M, Nastou K, Mehryary F, Hachilif R, *et al*. The STRING database in 2023: protein-protein association networks and functional enrichment analyses for any sequenced genome of interest. Nucleic Acids Research. 2023; 51: D638–D646. https://doi.org/10.1093/nar/gkac1000.

[33] Subramanian A, Tamayo P, Mootha VK, Mukherjee S, Ebert BL, Gillette MA, *et al*. Gene set enrichment analysis: a knowledge-based approach for interpreting genome-wide expression profiles. Proceedings of the National Academy of Sciences of the United States of America. 2005; 102: 15545–15550. https://doi.org/10.1073/pnas.0506580102.

[34] Chen B, Khodadoust MS, Liu CL, Newman AM, Alizadeh AA. Profiling Tumor Infiltrating Immune Cells with CIBERSORT. Methods in Molecular Biology (Clifton, N.J.). 2018; 1711: 243–259. https://doi.org/10.1007/978-1-4939-7493-1_12.

[35] Sun D, Wang J, Han Y, Dong X, Ge J, Zheng R, *et al*. TISCH: a comprehensive web resource enabling interactive single-cell transcriptome visualization of tumor microenvironment. Nucleic Acids Research. 2021; 49: D1420–D1430. https://doi.org/10.1093/nar/gkaa1020.

[36] Yang W, Soares J, Greninger P, Edelman EJ, Lightfoot H, Forbes S, *et al*. Genomics of Drug Sensitivity in Cancer (GDSC): a resource for therapeutic biomarker discovery in cancer cells. Nucleic Acids Research. 2013; 41: D955–61. https://doi.org/10.1093/nar/gks1111.

[37] Fu J, Li K, Zhang W, Wan C, Zhang J, Jiang P, *et al*. Large-scale public data reuse to model immunotherapy response and resistance. Genome Medicine. 2020; 12: 21. https://doi.org/10.1186/s13073-020-0721-z.

[38] Yang Y, Chen D, Liu H, Yang K. Increased expression of lncRNA CASC9 promotes tumor progression by suppressing autophagy-mediated cell apoptosis via the AKT/mTOR pathway in oral squamous cell carcinoma. Cell Death & Disease. 2019; 10: 41. https://doi.org/10.1038/s41419-018-1280-8.

[39] Mirabello L, Troisi RJ, Savage SA. Osteosarcoma incidence and survival rates from 1973 to 2004: data from the Surveillance, Epidemiology, and End Results Program. Cancer. 2009; 115: 1531–1543. https://doi.org/10.1002/cncr.24121.

[40] Chen XY, Ruan HB, Long XH, Peng AF, Zhou LD, Liu JM, *et al*. Blocking fatty acid synthase inhibits tumor progression of human osteosarcoma by regulating the human epidermal growth factor receptor 2/phosphoinositide 3-kinase/protein kinase B signaling pathway in xenograft models. Experimental and Therapeutic Medicine. 2017; 13: 2411–2416. https://doi.org/10.3892/etm.2017.4284.

[41] Meazza C, Asaftei SD. State-of-the-art, approved therapeutics for the pharmacological management of osteosarcoma. Expert Opinion on Pharmacotherapy. 2021; 22: 1995–2006. https://doi.org/10.1080/14656566.2021.1936499.

[42] Zhang K, Lu S, Jiang M, Zou X, Chen C, Lan Y, *et al*. Development of a Risk Model and Genotyping Patterns Based

on Disulfidptosis-Related lncRNAs to Predict Prognosis and Immune Landscape in Osteosarcoma. Frontiers in Bioscience (Landmark Edition). 2024; 29: 193. https://doi.org/10.31083/j.fbl2905193.

[43] Li G, Feng J, Huang S, Li Q. LncRNA-PVT1 Inhibits Ferroptosis through Activating STAT3/GPX4 Axis to Promote Osteosarcoma Progression. Frontiers in Bioscience (Landmark Edition). 2024; 29: 207. https://doi.org/10.31083/j.fbl2906207.

[44] Qiao Z, Li J, Kou H, Chen X, Bao D, Shang G, *et al*. Hsa-miR-557 Inhibits Osteosarcoma Growth Through Targeting KRAS. Frontiers in Genetics. 2022; 12: 789823. https://doi.org/10.3389/fgene.2021.789823.

[45] Zhang S, Hou C, Li G, Zhong Y, Zhang J, Guo X, *et al*. A single nucleotide polymorphism in the 3'-untranslated region of the KRAS gene disrupts the interaction with let-7a and enhances the metastatic potential of osteosarcoma cells. International Journal of Molecular Medicine. 2016; 38: 919–926. https://doi.org/10.3892/ijmm.2016.2661.

[46] Korzeniecki C, Priefer R. Targeting KRAS mutant cancers by preventing signaling transduction in the MAPK pathway. European Journal of Medicinal Chemistry. 2021; 211: 113006. https://doi.org/10.1016/j.ejmech.2020.113006.

[47] Stark GR, Taylor WR. Analyzing the G2/M checkpoint. Methods in Molecular Biology (Clifton, N.J.). 2004; 280: 51–82. https://doi.org/10.1385/1-59259-788-2:051.

[48] Smith HL, Southgate H, Tweddle DA, Curtin NJ. DNA damage checkpoint kinases in cancer. Expert Reviews in Molecular Medicine. 2020; 22: e2. https://doi.org/10.1017/erm.2020.3.

[49] Wang H, Zhang T, Sun W, Wang Z, Zuo D, Zhou Z, *et al*. Erianin induces G2/M-phase arrest, apoptosis, and autophagy via the ROS/JNK signaling pathway in human osteosarcoma cells in vitro and in vivo. Cell Death & Disease. 2016; 7: e2247. https://doi.org/10.1038/cddis.2016.138.

[50] Zhou B, Lin W, Long Y, Yang Y, Zhang H, Wu K, *et al*. NOTCH signaling pathway: architecture, disease, and therapeutics. Signal Transduction and Targeted Therapy. 2022; 7: 95. https://doi.org/10.1038/s41392-022-00934-y.

[51] Zhang Z, Wu W, Shao Z. NOTCH Signaling in Osteosarcoma. Current Issues in Molecular Biology. 2023; 45: 2266–2283. https://doi.org/10.3390/cimb45030146.

[52] Nirala BK, Yamamichi T, Yustein JT. Deciphering the Signaling Mechanisms of Osteosarcoma Tumorigenesis. International Journal of Molecular Sciences. 2023; 24: 11367. https://doi.org/10.3390/ijms241411367.

[53] McManus MM, Weiss KR, Hughes DPM. Understanding the role of NOTCH in osteosarcoma. Advances in Experimental Medicine and Biology. 2014; 804: 67–92. https://doi.org/10.1007/978-3-319-04843-7_4.

[54] Peng D, Fu M, Wang M, Wei Y, Wei X. Targeting TGF-β signal transduction for fibrosis and cancer therapy. Molecular Cancer. 2022; 21: 104. https://doi.org/10.1186/s12943-022-01569-x.

[55] Lamora A, Talbot J, Mullard M, Brounais-Le Royer B, Redini F, Verrecchia F. TGF-β Signaling in Bone Remodeling and Osteosarcoma Progression. Journal of Clinical Medicine. 2016; 5: 96. https://doi.org/10.3390/jcm5110096.

[56] McKinstry KK, Strutt TM, Swain SL. The effector to memory transition of CD4 T cells. Immunologic Research. 2008; 40: 114–127. https://doi.org/10.1007/s12026-007-8004-y.

[57] Lenardo MJ. Molecular regulation of T lymphocyte homeostasis in the healthy and diseased immune system. Immunologic Research. 2003; 27: 387–398. https://doi.org/10.1385/IR:27:2-3:387.

[58] Gu-Trantien C, Willard-Gallo K. Tumor-infiltrating follicular helper T cells: The new kids on the block. Oncoimmunology. 2013; 2: e26066. https://doi.org/10.4161/onci.26066.

[59] Jiang P, Gu S, Pan D, Fu J, Sahu A, Hu X, *et al*. Signatures of T cell dysfunction and exclusion predict cancer immunotherapy response. Nature Medicine. 2018; 24: 1550–1558. https://doi.org/10.1038/s41591-018-0136-1.

[60] Montemurro F, Valabrega G, Aglietta M. Lapatinib: a dual inhibitor of EGFR and HER2 tyrosine kinase activity. Expert Opinion on Biological Therapy. 2007; 7: 257–268. https://doi.org/10.1517/14712598.7.2.257.

[61] Hisamatsu Y, Oki E, Otsu H, Ando K, Saeki H, Tokunaga E, *et al*. Effect of EGFR and p-AKT Overexpression on Chromosomal Instability in Gastric Cancer. Annals of Surgical Oncology. 2016; 23: 1986–1992. https://doi.org/10.1245/s10434-016-5097-3.